PAPER

Check for updates

Shine-through luminescent wood membranes†

Maximilian Ritter, [ID] [ab] Ingo Burgert [ID] [ab] and Guido Panzarasa [ID] *[a]

Thanks to its optical anisotropy and mechanical properties, luminescent wood is a promising material for indoor lighting applications. However, the state-of-the-art approaches make use of potentially toxic fluorophores and of non-biodegradable polymers to increase the transparency, compromising the otherwise excellent sustainability of wood. Moreover, these procedures require lengthy multistep functionalisation processes and often fail to preserve the natural aesthetics of wood. We took advantage of the intrinsically hierarchical structure of wood coupling it with an efficient fluorophore, europium dibenzoylmethide triethylammonium (EuD$_3$TEA), to achieve uniform illumination *via* a shine-through effect. A safe, low-power near-UV LED was used to excite the europium complex, and the light emitted was transmitted through the wood scaffold. We explored the effect of different wood cutting directions, as well as of lignin decolourisation. The optical transmission was the highest for cross-section cuts and could be further increased by decolourisation. Our approach is simple, sustainable and fully preserves the aesthetic appearance of natural wood. Moreover, thanks to the pH-responsiveness of EuD$_3$TEA photoluminescence, the resulting luminescent wood could be used as a sensor for acidic or alkaline vapours.

Introduction

Addressing the current environmental challenges requires the substitution of conventional fossil-based materials with more sustainable and CO_2-storing ones. This is especially important for the building sector, which is responsible for one of the largest shares of total CO_2 emissions.[1,2] Conventional buildings require huge amounts of unsustainable materials, including those for lighting applications. Due to the impact on the global climate of the building sector for the growing human population, there is an urgent need to find and apply more sustainable solutions.[3–5] Wood is a state-of-the-art building material, with excellent mechanical properties, and prone to further functionalisation thanks to its multiscale porosity and ready availability of hydroxyl groups from the cellulose backbone. Furthermore, it is an intrinsically sustainable and CO_2-storing natural resource.[6] Enabling wood with new functionalities, including visual environmental responsiveness,[7] is an important factor to promote its widespread use in buildings beyond conventional structural applications.[6,8–12] Luminescent wood has recently caught considerable attention as an attractive

substitute for more conventional materials for indoor and outdoor lighting applications, such as brittle glass and non-biodegradable plastics, thanks to the sustainability and promising anisotropic optical properties of wood.[7,13–17] However, state-of-the-art wood-based lighting appliances require lengthy procedures for their preparation, including delignification and impregnation with often non-biodegradable polymers to improve the matrix transparency, and the use of potentially toxic fluorophores. These approaches compromise the intrinsic sustainability of wood[7,13] as well as the native woods' valuable aesthetic appearance, a detail of not negligible importance since it has been demonstrated that the use of natural wood in buildings can have positive effects on the wellbeing of inhabitants.[18] Although wood is intrinsically fluorescent due to lignin (Fig. S1, ESI†), this emission of light is too weak to be exploited for practical lighting applications.[19] Furthermore, natural wood is a rather opaque material. Light extinction in wood happens both as a result of scattering from cellulose fibres and absorption by lignin chromophores.[19,20,21] Delignification, however, could reduce the mechanical stability of wood, while selectively removing lignin's chromophores ("bleaching") can improve the optical qualities of wood without affecting its structural stability to the same degree.[22,23] The structural anisotropy of wood, with its nano- and micro-channel structure in the longitudinal direction, allows light-guiding thanks to direct transmission and scattering effects. Here we take advantage of these intrinsic features of wood membranes to propose a new one-step approach towards

[a] Wood Materials Science, Institute for Building Materials, ETH Zürich, 8093 Zürich, Switzerland. E-mail: guido.panzarasa@ifb.baug.ethz.ch

[b] WoodTec group, Cellulose and Wood Materials, Empa – Swiss Federal Laboratories for Materials Science and Technology, 8600 Dübendorf, Switzerland

† Electronic supplementary information (ESI) available: Full experimental details, additional results and images. See DOI: 10.1039/d1ma01045j

luminescent wood. Compared to the state-of-the-art, our approach preserves the intrinsic sustainability and aesthetics of wood to a greater extent, is highly efficient and environmentally friendly, and more easily scalable.

Results and discussion

Spruce is one of the wood species most widely available and used for building purposes in Europe[24] and, as such, we chose it as the starting material of our investigations. Due to the highly anisotropic structure of wood, it stands to reason that the wood–light interaction would be drastically different depending on the orientation of pores (cell lumina) relative to the incoming light direction. Samples of spruce wood with comparable thickness ($\sim$1 mm, Table S1, ESI†) were prepared in three different cutting directions, namely: cross-section (C), radial (R) and tangential (T), and their light transmission profiles were measured (Fig. 1A). For all samples, the transmission is highest for light above 700 nm, while UV light is almost completely blocked. The intensity of transmitted light, on the other hand, is highly dependent on the cutting direction. The transmission of the cross-section is approx. Two times the transmission of the tangential cut, which in turn is also almost two times that of the radial cut. The increased transmission of the cross-sections is due to the majority of the light passing through the cell lumina (average diameter in spruce

about 25 μm[25]), while in tangential and radial cuts, light has to pass multiple cell walls, resulting in higher absorption. In the wood cell walls, lignin is mainly responsible for light absorption. The removal of lignin chromophores by chemical bleaching (Fig. S2, based on the approach described by Li et al.,[23] full experimental details in the ESI†) increased the intensity of transmitted light below 600 nm dramatically (Fig. 1A). These differences are further depicted in Fig. 1B–E, which show images of the transmission of a light source through a native and a decolourised wood cross-section (Fig. 1B and C) and a radial cut of native and decolourised wood (Fig. 1D and E). Further increasing the light transmission would require a multi-step approach, first to delignify the wood scaffold and then to impregnate it with an index-matching polymer (such as PMMA), leading to conventional "transparent wood". Otherwise, the membrane thickness could be reduced, but the mechanical resistance would decrease as well. Decolourisation is not only simpler (as it requires only one step), it also improves the optical properties of wood while preserving the mechanical properties to a good extent (Fig. S3, ESI†). The tensile strength (tested in the tangential direction) decreased from 2.7 N mm^{-2} for native spruce (in agreement with typical values for tensile strength perpendicular to the grain direction[26]) to 1.4 N mm^{-2} for decolourised spruce. Whilst the ultimate elongation does not change significantly, the Young's modulus decreased from 287 N mm^{-2} to 197 N mm^{-2}. Nevertheless, decolourised wood is still more mechanically stable perpendicular to the fibre direction than its fully delignified counterpart.

Building on these results, we demonstrate the convenient fabrication of free-standing luminescent wood membranes for indoor lighting applications, based on the shine-through approach. A millimetre-thick wood veneer is functionalised on one side with a fluorophore, which is excited by direct irradiation with a near-UV source. The emitted light is guided through the wood matrix and emerges from the opposite side, while UV light is completely blocked (Fig. 1F).

As a fluorophore, we chose europium dibenzoylmethide triethylammonium (EuD$_3$TEA, Fig. 2A), which emits bright red light when exposed to near-UV light.[27–31] Europium β-diketonate complexes are well-known for their excellent photophysical properties, and environment friendliness.[27–29,32,33] Moreover, the fluorescence of EuD$_3$TEA is pH-responsive.[30,33] Additionally, the functionalisation with EuD$_3$TEA preserves wood's natural aesthetics. The importance of this latter quality is highlighted by a parallel set of experiments (pages S12–S16, Fig. S12–S18, ESI†) with fluorescein, a common organic fluorophore that shares all the previously mentioned properties with EuD$_3$TEA, but causes significant discolouration of the wood substrate. We synthesised EuD$_3$TEA according to the protocol given by Fontenot et al.[34] and used it to functionalise wood samples by dropping or spraying on them a fixed volume of 10 mM EuD$_3$TEA solution in ethanol and leaving it to dry (the resulting ATR-FTIR spectra of the samples are shown in Fig. S4, ESI†). Fig. 2B shows the appearance of a 4 × 4 cm^2 native spruce cross-section functionalised with EuD$_3$TEA illuminated
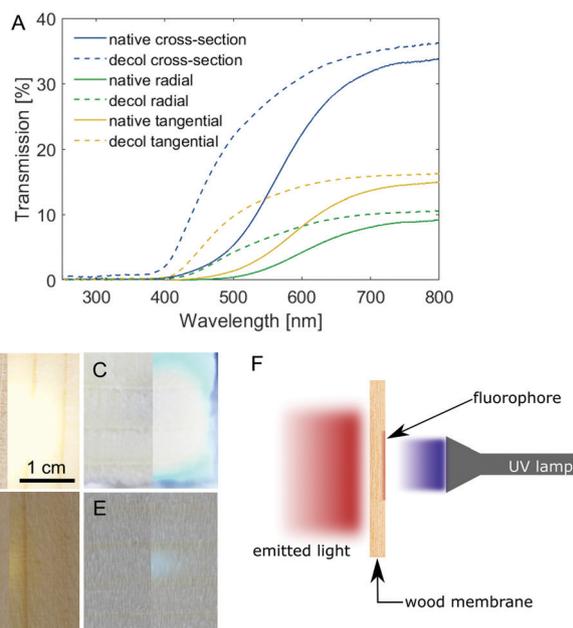

Fig. 1 (A) Transmission of light through different native (*full lines*) and decolourised (*dotted lines*) cuts of wood with comparable thickness: cross-section (*blue line*), radial cut (*green line*) and tangential cut (*yellow line*). (B–E) Visualisation of the difference in transmission between a native cross-section (B), decolourised cross-section (C), native radial cut (D) and decolourised radial cut (E). The *left* side of the image is not illuminated, the *right* side is illuminated from the bottom. (F) Schematic representation of the shine-through approach.
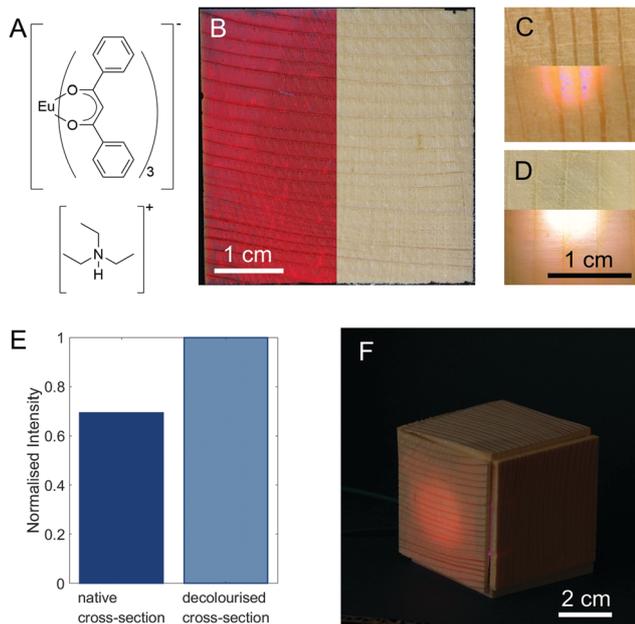
Fig. 2 (A) Schematic representation of the EuD$_3$TEA complex. (B) Functionalised cross-section illuminated by 366 nm UV light (*left*) and illuminated by daylight (*right*). (C) EuD$_3$TEA functionalised native cross-section (10 µL dropped on top) illuminated with UV light from the bottom (*bottom*) vs not illuminated (*top*). (D) EuD$_3$TEA functionalised decolourised cross-section illuminated with a 395 nm UV light from the bottom (*bottom*) and not illuminated (*top*). In both I and J the illuminated area is a circle with a ~3 mm diameter. (E) Quantification of the shine through intensity (based on the main emission peak, $\lambda_{em,max}$ ~615 nm) of EuD$_3$TEA functionalised native (*full blue bar*) and decolourised (*faint blue bar*) spruce (λ_{ex} = 375 nm). (F) Wooden cube (approx. 4 × 4 × 4 cm^3) with five native spruce cross-section faces (thickness >2.3 mm) and one EuD$_3$TEA functionalised cross-section face (membrane thickness 1.59 mm) illuminated by a 375 nm UV LED on the inside.

scalability, as cross-sections are more limited in size than radial and tangential cuts.

To better highlight the performance of our fluorescent shine-through wood membrane, we built a demonstrator (Fig. 2F) with five 4 × 4 cm^2 native spruce membranes and the fluorescent membrane shown in Fig. 2B arranged in the shape of a cube around a UV LED (λ_{ex} = 375 nm) pointing towards the fluorescent face. A single LED is enough to illuminate the entire fluorescent membrane. Full details of the demonstrator's construction, as well as an image of the demonstrator with a fluorescent decolourised wood face (Fig. S7, ESI†) are available in the ESI.† The shine-through luminescence, demonstrated here on a small scale, could be scaled up and applied to building walls and ceilings for lighting and design applications, especially considering the easy scalability of the functionalisation steps. By functionalising the wood membranes with different fluorophores, a range of colours may be realised. Additionally, the scattering of light in the wood reduces the amount of UV LEDs necessary for continuous illumination. Furthermore, by treating the individual LEDs as individual pixels, it would be possible to use large walls of luminescent wood as "displays".

It is worth noting here that the fluorescence behaviour of EuD$_3$TEA is pH-responsive.[30,31] By changing the pH of the fluorophore's environment, its fluorescence will either increase or decrease. To take advantage of this behaviour, we studied the evolution of the fluorescence response as a function of exposure of the fluorescent wood to acidic and alkaline vapours. Fig. 3 gives a comprehensive overview of the pH response of
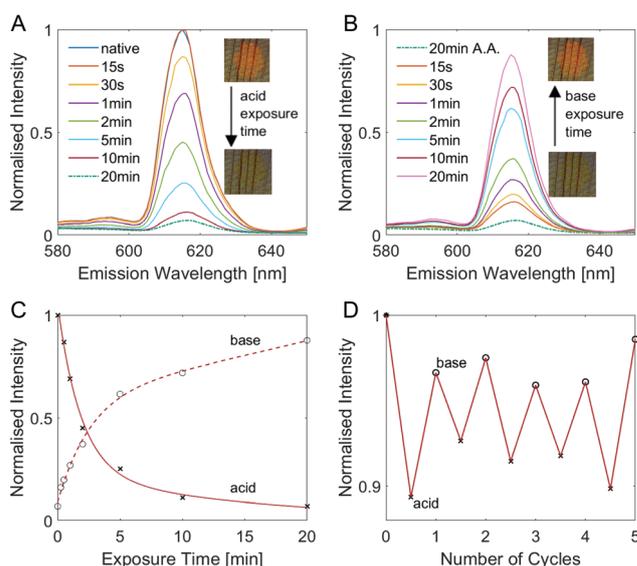
from above with UV light (λ_{ex} = 366 nm, left) and visible light (right). One of the main advantages of EuD$_3$TEA is that it does not alter the aesthetics of wood. By illuminating the functionalised side directly with a UV light source, the red-light emission can be detected on the opposite side. This is shown for a functionalised native and decolourised spruce cross-section in Fig. 2C and D respectively. The scattering of light in wood leads to a larger area emitting light than the area that is illuminated, ensuring a highly uniform illumination. Already from a qualitative comparison between these two images, it is possible to appreciate the higher intensity of the light emission from decolourised wood (Fig. 2D) compared to that from the native one (Fig. 2C).

The effect is quantified in Fig. 2E by comparing the intensity of the main emission peak ($\lambda_{em,max}$ ~615 nm) of the EuD$_3$TEA spectrum (the full spectrum is shown in Fig. S5, ESI,† the thickness of the samples is given in Table S2, ESI† and is approx. 1 mm). For decolourised wood, the fluorescence intensity is increased by a factor of about 1.4. Thanks to decolourisation, both radial and tangential cuts show sufficient performance in the shine-through setup (as shown in Fig. S6, ESI†). This is of special relevance for

Fig. 3 Fluorescence of EuD$_3$TEA-functionalised native wood cross-sections exposed to acetic and alkaline vapours. (A) The main emission peak of EuD$_3$TEA (~615 nm) in native wood as a function of time exposed to acetic acid (A.A.) vapour. (B) The main emission peak of EuD$_3$TEA as a function of time exposed to Et$_3$N vapour. (C) The intensity of the main emission peak plotted against the acetic acid (*crosses*) and Et$_3$N (*circles*) exposure time and fitted with an exponential approach (full red line for acetic acid and dotted red line for Et$_3$N). (D) The intensity after alternating 1 min exposure to acetic acid (*cross*) and Et$_3$N (*circle*) vapours.

native EuD$_3$TEA-functionalised spruce wood. The equivalent plots are shown for decolourised EuD$_3$TEA-functionalised wood in Fig S8 (ESI†). The longer the time for which EuD$_3$TEA-functionalised wood is exposed to acetic acid (A.A.) vapours, the less intense the fluorescence becomes, as shown in a Fig. 3 plot of intensity against time. Fig. 3C shows the exponential nature of the pH-response. This behaviour shows good reproducibility and can be repeated for many cycles. Exposing a sample alternatively to acetic acid and Et$_3$N vapours for 1 min each leads to a detectable fluorescence increase and decrease, respectively. This cycle can be performed at least five times without negatively affecting the performance (Fig. 3D). A. For both native and decolourised wood, the fluorescence decreases by approx. 90% after 20 minutes of acetic acid vapour exposure. Longer exposure times did not lead to an additional decrease (as can be seen by comparing the fluorescence intensity after 20 and 100 minutes in Fig. 3A). Fluorescence could then be restored by exposing the sample to triethylamine (Et$_3$N) vapours. Interestingly, native and decolourised wood reacted differently. The native wood recovered its fluorescence intensity much faster ($\sim$90% after 20 minutes, Fig. S8B, ESI†) than the decolourised one (only $\sim$60% after 20 minutes, Fig. 3B). This different behaviour might be explained by the contribution of fluorophores from inside the bulk, which need more time to be reached by the vapour diffusing in the bulk of wood. A plot of the fluorescence intensity against time (Fig. 3C) shows the exponential nature of the pH-response. This behaviour shows good reproducibility and can be repeated for many cycles. Exposing a sample alternatively to acetic acid and Et$_3$N vapours for 1 min each leads to a detectable fluorescence increase and decrease, respectively. This cycle can be performed at least five times without negatively affecting the performance (Fig. 3D).

As shown in Fig. S9 (ESI†), comparable results can be obtained with inorganic acids and bases, like hydrochloric acid HCl and ammonia NH$_3$. Using this couple, dramatic changes in the fluorescence intensity can be observed for even shorter exposure times as both are considerably stronger than their organic counterparts, acetic acid and Et$_3$N. This pH-dependent fluorescence could be used as an optical indicator of indoor air quality, especially in industrial and farming settings.

The photostability of the luminescent EuD$_3$TEA-functionalised wood was evaluated by accelerated ageing. As shown in Fig. S10 (ESI†), after 5 h of exposure to 1000 W m^{-2} UV light (corresponding to about 45 h of continuous exposure to direct sunlight), the fluorescence was reduced to 20% compared to the initial conditions. Fig. S11 (ESI†) shows the associated changes in the ATR-FTIR spectra.

Conclusions

We demonstrated a new environmentally friendly approach to make luminescent wood. We took advantage of wood's hierarchical structure to achieve a shine-through effect and applied it to a highly efficient fluorophore (EuD$_3$TEA) with pH-responsive fluorescence. Our luminescent wood retains its visual appeal under ambient light but glows red when illuminated with UV light. The shine-through effect was achieved using cross-sections as the most efficient light-transmitting wood cuts. We demonstrated that, thanks to wood decolourisation, other more scalable wood cuts could be used as well. Eventually, we proposed a possible application for our luminescent wood as an indoor air quality indicator. The scalability of the process and the good mechanical properties of the resulting wood membranes make our single-step approach highly promising for large-scale fabrication of indoor lighting appliances.

Conflicts of interest

There are no conflicts to declare.

Acknowledgements

Notes and references

1 I. E. A. IEA, Energy, technology, perspectives 2008: scenarios & strategies to 2050: in support of the G8 plan of action, Paris, 2008.

2 J. M. Allwood, *Sustainable Materials: With Both Eyes Open*, Cambridge: UIT, Cambridge, 2012.

3 D. B. Müller, G. Liu, A. N. Løvik, R. Modaresi, S. Pauliuk, F. S. Steinhoff and H. Brattebø, *Environ. Sci. Technol.*, 2013, **47**, 11739–11746.

4 G. Churkina, A. Organschi, C. P. O. Reyer, A. Ruff, K. Vinke, Z. Liu, B. K. Reck, T. E. Graedel and H. J. Schellnhuber, *Nat. Sustainable*, 2020, **3**, 269–276.

5 V. Masson-Delmotte, P. Zhai, H.-O. Pörtner, D. Roberts, J. Skea, P. R. Shukla, A. Pirani, W. Moufouma-Okia, C. Péan, R. Pidcock, S. Connors, J. B. R. Matthews, Y. Chen, X. Zhou, M. I. Gomis, E. Lonnoy, T. Maycock, M. Tignor, and T. Waterfield, ed., *IPCC, Summary for Policymakers. In: Global Warming of 1.5 °C. An IPCC Special Report on the impacts of global warming of 1.5 °C above pre-industrial levels and related global greenhouse gas emission pathways, in the context of strengthening the global response tothe threat of climate change, sustainable development,and efforts to eradicate poverty*, 2018.

6 L. A. Berglund and I. Burgert, *Adv. Mater.*, 2018, **30**, 1–15.

7 Y. Liu, H. Yang, C. Ma, S. Luo, M. Xu, Z. Wu, W. Li and S. Liu, *ACS Appl. Mater. Interfaces*, 2020, **12**, 36628–36638.

8 F. Jiang, T. Li, Y. Li, Y. Zhang, A. Gong, J. Dai, E. Hitz, W. Luo and L. Hu, *Adv. Mater.*, 2018, **30**, 1–39.

9 J. Sun, H. Guo, G. N. Schädli, K. Tu, S. Schär, F. W. M. R. Schwarze, G. Panzarasa, J. Ribera and I. Burgert, *Sci. Adv.*, 2021, **7**, eabd9138.

10 J. Sun, H. Guo, J. Ribera, C. Wu, K. Tu, M. Binelli, G. Panzarasa, F. W. M. R. Schwarze, Z. L. Wang and I. Burgert, *ACS Nano*, 2020, **14**, 14665–14674.

11 C. Goldhahn, J. A. Taut, M. Schubert, I. Burgert and M. Chanana, *RSC Adv.*, 2020, **10**, 20608–20619.

12 Y. Ding, K. Tu, I. Burgert and T. Keplinger, *J. Mater. Chem. A*, 2020, **8**(42), 22001–22008.

13 Q. Fu, I. Burgert, K. Tu, C. Goldhahn, T. Keplinger, M. Adobes-Vidal and M. Sorieul, *ACS Nano*, 2020, **14**, 13775–13783.

14 X. Li, Y. Li, Y. Luo, Q. Mou, X. Li, L. Xie and Y. Wu, *J. Nanomater.*, 2014, **2014**, 1–4.

15 E. Vasileva, Y. Li, I. Sychugov, M. Mensi, L. Berglund and S. Popov, *Adv. Opt. Mater.*, 2017, **5**, 1–6.

16 K. Fanru, H. Rui, W. Di and L. Jian, *Mater. Res.*, 2019, **22**, e20180712.

17 D. Van Opdenbosch, M. H. Kostova, S. Gruber, S. Krolikowski, P. Greil and C. Zollfrank, *Wood Sci. Technol.*, 2010, **44**, 547–560.

18 K. Strobel, A. Q. Nyrud and K. Bysheim, *Scand. J. For. Res.*, 2017, **32**, 798–806.

19 B. Albinsson, S. Li, K. Lundquist and R. Stomberg, *J. Mol. Struct.*, 1999, **508**, 19–27.

20 U. Müller, M. Rätzsch, M. Schwanninger, M. Steiner and H. Zöbl, *J. Photochem. Photobiol. B*, 2003, **69**, 97–105.

21 M. M. Caldwell, L. O. Björn, J. F. Bornman, S. D. Flint, G. Kulandaivelu, A. H. Teramura and M. Tevini, *J. Photochem. Photobiol. B*, 1998, **46**, 40–52.

22 Q. Xia, C. Chen, Y. Yao, S. He, X. Wang, J. Li, J. Gao, W. Gan, B. Jiang, M. Cui and L. Hu, *Adv. Mater.*, 2021, **2001588**, 1–10.

23 Y. Li, Q. Fu, R. Rojas, M. Yan, M. Lawoko and L. Berglund, *ChemSusChem*, 2017, **10**, 3445–3451.

24 G. Caudullo, W. Tinner and D. de Rigo, *Eur. Atlas For. Tree Species.*, 2016, 114–116.

25 I. Irbe, I. Sable, G. Noldt, U. Grinfelds, A. Jansons, A. Treimanis and G. Koch, *Balt. For.*, 2015, **21**, 114–123.

26 Forest Products Laboratory – USDA, USDA – Gen. Tech. Rep.

27 R. S. Fontenot, K. N. Bhat, W. A. Hollerman and M. D. Aggarwal, *Mater. Today*, 2011, **14**, 292–293.

28 C. R. Hurt, N. McAvoy, S. Bjorklund and N. Filipescu, *Nature*, 1966, **212**, 179–180.

29 R. S. Fontenot, W. A. Hollerman, K. N. Bhat and M. D. Aggarwal, *J. Lumin.*, 2012, **132**, 1812–1818.

30 S. Blair, M. P. Lowe, C. E. Mathieu, D. Parker, P. K. Senanayake and R. Kataky, *Inorg. Chem.*, 2001, **40**, 5860–5867.

31 X. Shen and B. Yan, *J. Mater. Chem. C*, 2015, **3**, 7038–7044.

32 Q. Xu, Z. Li and H. Li, *Chem. – Eur. J.*, 2016, **22**, 3037–3043.

33 F. S. Richardson, *Chem. Rev.*, 1982, **82**, 541–552.

34 R. S. Fontenot, K. N. Bhat, W. A. Hollerman and M. D. Aggarwal, *Mater. Today*, 2011, **14**, 292–293.